Applied Physics Letters ARTICLE pubs.aip.org/aip/apl

Comparative study of the interface passivation properties of LiF and Al_2O_3 using silicon MIS capacitor

Cite as: Appl. Phys. Lett. **124**, 142901 (2024); doi: 10.1063/5.0203484
Submitted: 14 February 2024 · Accepted: 22 March 2024 ·
Published Online: 2 April 2024

Jonathan Parion,[1,2,3,a)] Romain Scaffidi,[1,2,3,4] Filip Duerinckx,[2,3] Hariharsudan Sivaramakrishnan Radhakrishnan,[2,3] Denis Flandre,[4] Jef Poortmans,[1,2,3,5] and Bart Vermang[1,2,3]

AFFILIATIONS

[1]Hasselt University, Wetenschapspark 1, 3590 Diepenbeek, Belgium
[2]Imec division imo-imomec, Thor Park 8320, 3600 Genk, Belgium
[3]EnergyVille, Thorpark 8320, 3600 Genk, Belgium
[4]ICTEAM, UCLouvain, Place du Levant 3, 1348 Louvain-la-Neuve, Belgium
[5]ESAT, KU Leuven, Kasteelpark Arenberg 10, 3001 Leuven, Belgium

[a)]Author to whom correspondence should be addressed: jonathan.parion@hotmail.be

ABSTRACT

Lithium fluoride (LiF) is currently a very popular dielectric material used as a passivation or transport layer in a variety of applications, especially in high-efficiency solar cells. Despite this, its conduction properties and interface behavior with silicon remain largely unexplored. In this work, a LiF metal–insulator–semiconductor (MIS) structure is fabricated and characterized, and its properties are compared to the well-understood aluminum oxide (Al_2O_3) MIS structure. First, a higher current density in LiF compared to Al_2O_3 is highlighted, as well as its PN junction-like behavior with n-type silicon (n-Si), being rather unconventional for a dielectric layer. C–V measurements showcase the likely presence of an interface defect, causing an increase in the apparent doping and a shift in the flatband voltage V_{FB} by +70 meV. This defect is found to be of the acceptor type, which renders the interface fixed charge more negative and improves the field-effect passivation in the case of a negative Q_f. Finally, a density of interface states $D_{it} \approx 2 \times 10^{11}\ \mathrm{cm^{-2}\,eV^{-1}}$ was found for LiF/n-Si, which is a low value showing appropriate chemical passivation at the interface. Overall, this work enables us to shed more light on the interface properties of LiF on n-Si, which is an essential step toward its wider use in state-of-the-art solar cells and other silicon-based devices.

Lithium fluoride (LiF) was previously presented as a very good material to lower the work function of metallic electrodes in light-emitting devices, therefore improving their contact properties.[1–3] More recently, it was also successfully demonstrated as an efficient passivation and transport layer in state-of-the-art solar cells, achieving world-record efficiencies.[4–6] Moreover, the key role played by passivation in many silicon-based devices motivates the idea that LiF could be of great interest well beyond the LED and solar cell applications. Despite these promising aspects, the conduction and interface properties of LiF with silicon are to this day largely unexplored, which is a major bottleneck in using this material in a wider range of applications.

The objective of this work is to provide a better understanding of the interface properties of LiF on n-type silicon (n-Si) by comparing it to Al_2O_3. This choice is motivated by the excellent passivation properties of Al_2O_3 on silicon and the extensive knowledge gathered for this material, especially in the context of silicon solar cells. For this comparison, the well-known metal–insulator–semiconductor (MIS) architecture is used, as schematically represented in Fig. 1. For the LiF MIS, an n-type silicon wafer with resistivity of $\rho \approx 2\,\Omega\,\mathrm{cm}$ is used, similar to state-of-the-art silicon solar cells. The wafer is cleaned following a standard process, and a 20 nm layer of LiF is thermally evaporated on top. The front contact is achieved using a mercury (Hg) probe station. Aluminum is evaporated on the backside of the wafer to create an ohmic contact. The same procedure is followed for the Al_2O_3 MIS but with 20 nm of Al_2O_3 deposited on top of n-Si by thermal atomic layer deposition (ALD).

First, current–voltage (I–V) measurements are realized in the dark to assess the conduction properties of both materials. Then,

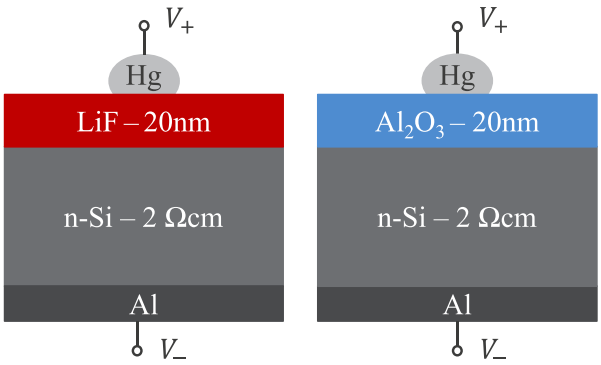

FIG. 1. Schematic representation of the devices used in this work. The front Hg contact (at the top) is realized with a mercury probe station, in which liquid mercury is brought in contact with the sample during the measurement and removed afterward. This takes place under vacuum and enables us to achieve optimal contact, without damaging the dielectric layer. The device active area is $A = 0.0065\,\mathrm{cm}^2$.

capacitance–voltage (C–V) and conductance–voltage (G–V) measurements are performed, also in the dark, to extract the interface and passivation properties of both materials.

I–V measurements are carried out in the dark, using a Keithley 2401 sourcemeter. Positive voltage is applied at the front, as shown in Fig. 1. The experimental J–V characteristics of both Al_2O_3 and LiF MIS stacks are shown in Fig. 2.

The current density in a MIS structure with a conventional dielectric is expected to be very low due to the wide bandgap of the material. It is dominated by ohmic conduction at low and reverse voltage biases, and by tunneling currents in larger forward bias. Typically, currents of the order of 10^{-5}–$10^{-3}\,\mathrm{mA/cm^2}$ can be observed in Al_2O_3/Si MIS capacitors under 1 V voltage bias, depending on the film thickness and the deposition process.[7,8] This appears to be in line with the observations in Fig. 2, where the current density for Al_2O_3 is about $3 \times 10^{-4}\,\mathrm{mA/cm^2}$ at 1 V. The low current density explains why Al_2O_3 transport layers are either very thin[9,10] or thicker and porous,[11,12] so as

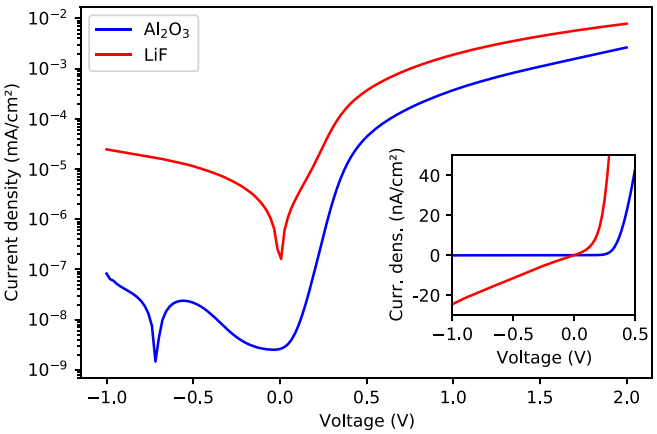

FIG. 2. Experimental current density characteristic for both Al_2O_3 and LiF structures presented in logarithmic scale. The behavior of these structures is represented in linear scale in the inset, highlighting the diode behavior of LiF more clearly.

to not significantly hinder the transport of charge carriers. This requirement is, however, not necessary when Al_2O_3 is used as a passivation layer, since the current does not directly flow through the layer itself.[13,14]

Compared to Al_2O_3, the current density for the LiF MIS displayed in Fig. 2 is noticeably higher, with a value of $2 \times 10^{-3}\,\mathrm{mA/cm^2}$ at 1 V. This could seem surprising, as the layers thicknesses are similar, and the bandgap of LiF ($E_g = 13$ eV) is far greater than the one of Al_2O_3 ($E_g = 6.2$ eV). However, such high current density in thick LiF layers was previously reported[15] and might be related to hopping conduction, in which carriers tunnel through defect states present in the dielectric film.[16] These conduction properties were also observed in thinner films[1–3] and should be, as mentioned earlier, beneficial in the case of a transport layer.

Conventional dielectrics, such as Al_2O_3, are in essence intrinsic layers without any form of doping. In LiF, on the contrary, the alleged bulk trap states might act as doping elements in the layer, therefore stepping away from the expected dielectric behavior. This hypothesis seems to be confirmed by the shape of the curve in Fig. 2, where LiF exhibits a very typical PN junction characteristic. The current density increases exponentially around 0 V and is negative in reverse bias, as clearly shown in the inset of Fig. 2. Also in reverse bias, the current is linear with respect to voltage with a steep decrease. This indicates a large minority carrier leakage current that is not observed for Al_2O_3 and might arguably have different contributions. Indeed, the possible presence of shunt paths in the LiF layer caused by localized pinholes, likely not present for the conformal ALD Al_2O_3 layer, or the impact of the LiF intrinsic doping may play a role, among others. This would require further investigations but is not considered to impede the presented analysis in the bias range of interest. The fact that LiF does not behave as a real dielectric but rather as a doped semiconductor layer is the first important sign of its unconventional properties and is taken into account when trying to apply the classical MIS theory in the following.

Interface properties of LiF and Al_2O_3 are extracted using C–V and G–V measurements. These are conducted using an HP 4284A LCR meter, with a positive voltage applied on the front contact (Fig. 1). The measurements are performed at 10 kHz, with a varying voltage between −0.5 and 2 V. Following the well-established theory of MIS capacitors,[17] the flatband voltage (V_{FB}) of the structure can be expressed as follows:

$$\frac{V_{FB}}{q} = \phi_{ms} - \frac{Q_f}{C_{ox}}, \tag{1}$$

where ϕ_{ms} is the contact potential difference, Q_f is the fixed charge at the dielectric interface, C_{ox} is the dielectric capacitance, and q is the elementary charge. In an ideal case where there is no interface charge, $q\phi_{ms} = V_{FB}$. In the presence of a fixed charge at the interface, the value of V_{FB} becomes greater or smaller if the charge sign is negative or positive, respectively, corresponding to a shift of the C–V characteristic in the rightward or leftward direction.[17] In an uniformly doped substrate, the experimental value of V_{FB} is extracted by taking the intercept between the horizontal axis and the linear region of the C^{-2} vs V plot.[18] The value of the apparent doping (N_D) is also extracted from the slope of that linear region, following the equation:

$$N_D = \frac{2}{q\varepsilon_r\varepsilon_0} \times \left(|slope|A^2\right), \tag{2}$$

where ε_r is the electrical permittivity of the semiconductor, ε_0 is the electrical permittivity of vacuum, and A is the gate area. The values of both V_{FB} and N_D were obtained for Al_2O_3 and LiF from the experimental C–V data and are shown in Fig. 3.

The C–V characteristic of the Al_2O_3 device, shown in the inset of Fig. 3, depicts the typical behavior of n-type MIS capacitors, with the accumulation region beyond 1 V and the depletion regime for negative or low forward bias. The value of apparent doping $N_D = 2 \times 10^{15}$ cm^{-3} extracted from the C^{-2} vs V characteristic (Fig. 3) comes rather close to the estimation $N_{D,th.} = 2.3 \times 10^{15}$ cm^{-3} based on the wafer resistivity $\rho_s \approx 2\,\Omega$ cm, which tends to confirm the applicability of the model for the Al_2O_3 structure. Subsequently, a value of flatband voltage $V_{FB} = 0.83$ V is obtained for Al_2O_3.

In the inset of Fig. 3, it appears that the C–V characteristic of the LiF device also presents two distinct regions similar to the Al_2O_3 structure. However, it exhibits a noticeable difference around 0.5 V, where the LiF curve shows a distinct peak emphasized by a black arrow. This feature most probably originates from an electronic defect.[19–21] When the applied voltage bias is varied, the position of the Fermi level in the bandgap changes, resulting in defect states being charged and discharged. In function of the defect type (bulk, interface) and its properties (activation energy, capture cross section), it contributes to the total measured capacitance of the device in a particular range of voltages. Interface defects, in particular, have a very limited span in terms of energy levels and, therefore charge and discharge themselves for a limited range of voltages. This results in a narrow response in the C–V plot, which is visibly the case in Fig. 3. This tends to indicate that the electronic defect is in fact an interface defect, most probably located at the interface between LiF and n-Si. It should be carefully considered when experimentally extracting the interface parameters, as it will likely influence the total charge and thus N_D, Q_f, and V_{FB}.

The interface defect produces a different pattern on the C^{-2} vs V characteristic, positioned around the same 0.5 V bias. Contrary to Al_2O_3, there are actually two distinct linear regions for LiF, yielding

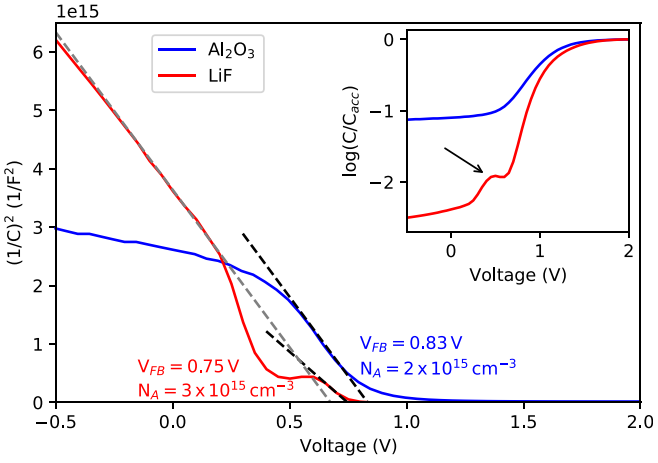

FIG. 3. Experimental C^{-2} vs V plot obtained from C–V measurements at 10 kHz. V_{FB} is extracted by extrapolation of the linear region of the C^{-2} vs V curve to the x-axis (black dashed lines). An additional line is represented in gray for LiF to highlight the impact of the interface defect on V_{FB}. The normalized C–V characteristic of both stacks is represented in log-scale in the top-right inset, and the response due to the interface defect identified for LiF is pointed with a black arrow.

different values of N_D and V_{FB}. The first one occurs before 0.4 V (gray dashed line—region 1) and the second one around 0.7–0.8 V (black dashed line—region 2), leading to $N_D = 2 \times 10^{15}$ and 3×10^{15} cm^{-3}, respectively. The value for N_D in region 1 is similar to the one obtained for Al_2O_3 (parallel intercept lines) and, thus, comparable to the theoretical doping of the wafer. This tends to indicate that the defect state would be depleted before 0.5 V and filled with charges after that, therefore contributing to the total apparent doping that is higher in region 2. Therefore, region 1 would be related to the intrinsic "defect-free" interface behavior between LiF and n-Si, and region 2 to a combination of both the intrinsic and interface defect contributions.

Due to the interface defect, there is a difference of +70 meV between the V_{FB} values that would be extracted in region 1 ($V_{FB} = 0.63$ V) and in region 2 ($V_{FB} = 0.75$ V). Following Eq. (1), an increase in V_{FB} within a single structure, where ϕ_{ms} and C_{ox} are constant, is necessarily caused by a more negative Q_f. This suggests that the additional charge generated by the interface defect states is negative, therefore pointing toward an acceptor-type defect.

When investigating the passivation properties of a dielectric material, two distinct mechanisms are considered. The first one is usually related to the fixed charge at the interface between the dielectric and the n-Si substrate (Q_f) and is called field-effect passivation.[17,22,23] Its magnitude and sign (positive or negative) depend on the interface defect density and type (donor or acceptor), respectively. Q_f is obtained as follows:[17]

$$Q_f = C_{ox} \times \left(\frac{V_{ms} - V_{FB}}{q} \right), \tag{3}$$

where $V_{ms} = q\phi_{ms}$. This equation is derived from Eq. (1) and is valid in the case of traditional dielectrics. For experimental data, V_{FB} is obtained as described in the previous paragraph, C_{ox} is extracted experimentally in the accumulation regime, and V_{ms} is computed as follows:

$$V_{ms} = V_m - \frac{1}{q}\left(\xi_{Si} + \frac{E_{g,Si}}{2} - (kT)\ln\left(\frac{N_D}{n_i}\right)\right), \tag{4}$$

where $V_m = 4.45$ V is the work function of the mercury probe, $\xi_{Si} = 4.05$ eV is the n-Si electron affinity, $E_{g,Si} = 1.12$ eV is the n-Si bandgap, $kT/q = 0.026$ eV is the thermal energy, and $n_i \approx 1.5 \times 10^{10}$ cm^{-3} is the intrinsic density of carriers in n-Si at room temperature.[24] Based on the previous computation and in the case of Al_2O_3, the interface fixed charge is $Q_f = -2.3 \times 10^{12}$ cm^{-2}, as also obtained in similar studies.[22,23,25] A negative fixed charge for a dielectric on a n-type Si wafer is useful at the low-potential side, since it facilitates the extraction of positive charge carriers (holes) when used as a transport layer.

The same methodology is not directly applicable for LiF, since it does not behave as an ideal dielectric in the same way as Al_2O_3 does. Due to its PN junction-like behavior with n-Si, it is not possible to accurately extract a value for Q_f. More precisely, the possible doping of the LiF layer introduces additional charges, which also influence the experimental Q_f value. This should, however, be confirmed by further investigation on the LiF layer itself, which is outside the scope of this work. Despite these uncertainties, it was previously shown that the interface defect is of acceptor type, thus, adding a negative charge to the interface. Depending on the "intrinsic" value of Q_f, this can either increase the field-effect passivation ($Q_f < 0$) or decrease it ($Q_f > 0$).

Based on the similarities between Al_2O_3 and LiF in terms of V_{FB}, it is reasonable to think that if Q_{f,Al_2O_3} is negative, so will $Q_{f,LiF}$ be. In that case, the interface defect actually strengthens the field-effect passivation, which is a beneficial feature of that defect.

The second passivation mechanism is related to the density of electronic defects at the n-Si interface (D_{it}) and is called chemical passivation.[17,22,23] Using Al_2O_3 to passivate the interface between n-Si and the neighboring electrical contact is greatly motivated by the subsequent reduction of D_{it} by one or even two orders of magnitude. A well-established technique to experimentally extract D_{it} is the conductance technique.[17] It is based on the evolution of the parallel conductance with voltage and frequency, which is obtained as follows:

$$\frac{G_p}{A\omega} = \frac{\omega G_m C_m^2}{G_m^2 + (\omega C_m)^2}, \tag{5}$$

where $\omega = 2\pi f$ is the angular frequency, C_m is the measured capacitance, and G_m is the measured conductance, both normalized by the area of the device. The capture and emission of charges by interface traps lead to a certain energy loss, which can be modeled by $G_p/A\omega$.[8] A peak in $G_p/A\omega$ with respect to voltage and frequency indicates the crossing of a defect state by the Fermi level in the same way as for the capacitance, both quantities being mathematically linked.[26] Based on this, the value of D_{it} can, therefore, be obtained by looking at the response peak, using the following equation:[17]

$$D_{it} = 2.5 \times \left(\frac{G_p/A\omega}{q}\right)_{\max}. \tag{6}$$

The $G_p/A\omega$ vs V characteristic is shown in Fig. 4. The most significant feature appearing in the $G_p/A\omega$ characteristic is the peak in conductance around 0.4 V in the LiF curve, which is likely caused by the interface defect identified before. At that voltage bias, the $G_p/A\omega$ response is about one order of magnitude greater for LiF than for Al_2O_3. It would be fair to question whether it is possible to compute a real value of D_{it} using $G_p/A\omega$, since it was previously shown to not behave as a real dielectric but rather as a PN junction. Several studies have previously used the conductance technique in MIS structures using non-conventional dielectrics and in PN junctions to extract D_{it}.[23,27–29] An

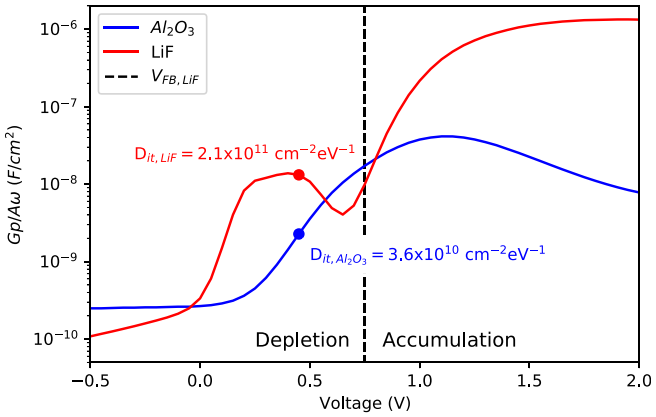

FIG. 4. Experimental $G_p/A\omega$ vs V plot obtained from G–V measurements at 10 kHz. The limit between the depletion and accumulation regime is represented for LiF. D_{it} is extracted in depletion for both dielectrics and represented in the figure.

important condition to this is that the D_{it} extraction is only valid in the depletion regime (low voltage bias) and not in the accumulation regime, where the conductance value might be altered by the large DC. In Fig. 4, the separation ($V = V_{FB}$) between depletion and accumulation for LiF is clearly demarcated by a black dashed line. In a similar fashion, when the reverse leakage current is high, care must also be taken on the interpretability of the results for negative voltage bias. The response for G_p/ω in reverse bias in Fig. 4 is not flat for LiF, contrarily to Al_2O_3, which is probably caused by the large reverse leakage current that was highlighted in the inset of Fig. 2. All in all, because the peak in conductance for LiF is situated in depletion regime, it is fair to assume that a plausible value of D_{it} can indeed be extracted, being $D_{it} \approx 2 \times 10^{11}$ cm^{-2} eV^{-1}. This is lower than for a direct electrical contact on silicon, thereby showing the good passivation properties of LiF. In the Al_2O_3 device at the same voltage bias, $D_{it} \approx 4 \times 10^{10}$ cm^{-2} eV^{-1}. The value of D_{it} is in this case not extracted at the peak position in voltage, because it is situated in the accumulation region, which does not satisfy the assumptions of Eq. (6). Moreover, the reported value is very close to the one reported in similar studies,[22,23,25] which justifies that it could constitute a good comparison point for the preceding analysis.

In this work, the interface passivation properties of LiF on n-Si are investigated and compared to those of Al_2O_3 using the well-known MIS architecture.

J–V measurements show a current density of 2×10^{-3} mA/cm^2 at 1 V for LiF, which is about 1 order of magnitude higher than that for Al_2O_3 and constitutes a real asset if LiF were to be used as a charge transport layer. These measurements also highlighted the unconventional dielectric behavior of LiF on n-Si, which is closer to that of a PN junction and might be explained by high doping in the LiF layer.

Using C–V measurements, the likely presence of an acceptor-type interface defect is identified, which results in an increase in the apparent doping from $N_D = 2 \times 10^{15}$ to 3×10^{15} cm^{-3} as well as in a rightward shift of V_{FB} by 70 meV. Moreover, this interface defect was proven to make the interface fixed charge more negative, which, in the case of a negative Q_f, strengthens the field-effect passivation.

Finally, G–V measurements and the associated $G_p/A\omega$ characteristics enable to extract an interface trap density value of $D_{it} \approx 2 \times 10^{11}$ cm^{-2} eV^{-1}, which is about 1 order of magnitude greater than Al_2O_3 at the same voltage bias but still very low to show good chemical passivation properties.

Overall, the comparison made in this work highlights the peculiar properties of LiF on n-Si compared to those of Al_2O_3. This should enable a better understanding of the material and its properties, thereby contributing to its wider adoption as the transport layer in n-type silicon solar cells and also in other silicon-based devices.

This study was supported by the Special Research Fund of Hasselt University, with No. BOF22OWB15. The authors thank the teams of the nanofabrication shared facility (WINFAB) and electrical characterization platform (WELCOME) at UCLouvain for their availability and technical support.

AUTHOR DECLARATIONS

Conflict of Interest

The authors have no conflicts to disclose.

Author Contributions

Jonathan Parion: Conceptualization (lead); Data curation (lead); Formal analysis (lead); Investigation (lead); Methodology (lead); Project administration (lead); Resources (lead); Software (lead); Supervision (lead); Validation (lead); Visualization (lead); Writing – original draft (lead); Writing – review & editing (equal). **Romain Scaffidi:** Formal analysis (supporting); Investigation (supporting); Validation (supporting); Visualization (supporting); Writing – review & editing (equal). **Filip Duerinckx:** Writing – review & editing (equal). **Hariharsudan Sivaramakrishnan Radhakrishnan:** Funding acquisition (equal); Writing – review & editing (equal). **Denis Flandre:** Funding acquisition (equal); Writing – review & editing (equal). **Jef Poortmans:** Funding acquisition (equal); Writing – review & editing (equal). **Bart Vermang:** Funding acquisition (equal); Writing – review & editing (equal).

DATA AVAILABILITY

The data that support the findings of this study are available from the corresponding author upon reasonable request.

REFERENCES

[1]M. G. Mason, C. W. Tang, L.-S. Hung, P. Raychaudhuri, J. Madathil, D. J. Giesen, L. Yan, Q. T. Le, Y. Gao, S.-T. Lee, L. S. Liao, L. F. Cheng, W. R. Salaneck, D. A. dos Santos, and J. L. Brédas, "Interfacial chemistry of Alq_3 and LiF with reactive metals," J. Appl. Phys. **89**, 2756–2765 (2001).

[2]T. M. Brown, R. H. Friend, I. S. Millard, D. J. Lacey, J. H. Burroughes, and F. Cacialli, "Efficient electron injection in blue-emitting polymer light-emitting diodes with LiF/Ca/Al cathodes," Appl. Phys. Lett. **79**, 174–176 (2001).

[3]T. M. Brown, R. H. Friend, I. S. Millard, D. J. Lacey, T. Butler, J. H. Burroughes, and F. Cacialli, "Electronic line-up in light-emitting diodes with alkali-halide/metal cathodes," J. Appl. Phys. **93**, 6159–6172 (2003).

[4]D. Menzel, A. Al-Ashouri, A. Tejada, I. Levine, J. A. Guerra, B. Rech, S. Albrecht, and L. Korte, "Field effect passivation in perovskite solar cells by a LiF interlayer," Adv. Energy Mater. **12**, 2201109 (2022).

[5]A. Al-Ashouri, E. Köhnen, B. Li, A. Magomedov, H. Hempel, P. Caprioglio, J. A. Márquez, A. B. M. Vilches, E. Kasparavicius, J. A. Smith, N. Phung, D. Menzel, M. Grischek, L. Kegelmann, D. Skroblin, C. Gollwitzer, T. Malinauskas, M. Jošt, G. Matič, B. Rech, R. Schlatmann, M. Topič, L. Korte, A. Abate, B. Stannowski, D. Neher, M. Stolterfoht, T. Unold, V. Getautis, and S. Albrecht, "Monolithic perovskite/silicon tandem solar cell with 29% efficiency by enhanced hole extraction," Science **370**, 1300–1309 (2020).

[6]M. Q. Khokhar, S. Q. Hussain, D. P. Pham, S. Lee, H. Park, Y. Kim, E.-C. Cho, and J. Yi, "Simulation of silicon heterojunction solar cells for high efficiency with lithium fluoride electron carrier selective layer," Energies **13**, 1635 (2020).

[7]J. Kolodzey, E. Chowdhury, T. Adam, G. Qui, I. Rau, J. Olowolafe, J. Suehle, and Y. Chen, "Electrical conduction and dielectric breakdown in aluminum oxide insulators on silicon," IEEE Trans. Electron Devices **47**, 121–128 (2000).

[8]Y. Yan, V. Kilchytska, B. Wang, S. Faniel, Y. Zeng, J.-P. Raskin, and D. Flandre, "Characterization of thin Al_2O_3/SiO_2 dielectric stack for CMOS transistors," Microelectron. Eng. **254**, 111708 (2022).

[9]J. Deckers, E. Cornagliotti, M. Debucquoy, I. Gordon, R. Mertens, and J. Poortmans, "Aluminum oxide-aluminum stacks for contact passivation in silicon solar cells," Energy Procedia **55**, 656–664 (2014).

[10]J. De Wild, G. Birant, G. Brammertz, M. Meuris, J. Poortmans, and B. Vermang, "Ultrathin $Cu(In,Ga)Se_2$ solar cells with Ag/AlO_x passivating back reflector," Energies **14**, 4268 (2021).

[11]I. Kandybka, G. Birant, J. De Wild, D. Buldu, T. Kohl, R. Thiruvallur Eachambadi, G. Brammertz, J. Manca, M. Meuris, J. Poortmans, and B. Vermang, "Novel cost-effective approach to produce nano-sized contact openings in an aluminum oxide passivation layer up to 30 nm thick for CIGS solar cells," J. Phys. D **54**, 234004 (2021).

[12]D. Buldu, J. De Wild, T. Kohl, G. Birant, G. Brammertz, M. Meuris, J. Poortmans, and B. Vermang, "A novel strategy for the application of an oxide layer to the front interface of $Cu(In,Ga)Se_2$ thin film solar cells: Al_2O_3/HfO_2 multi-stack design with contact openings," IEEE J. Photovoltaics **12**, 301 (2022).

[13]B. Vermang, H. Goverde, L. Tous, A. Lorenz, P. Choulat, J. Horzel, J. John, J. Poortmans, and R. Mertens, "Approach for Al_2O_3 rear surface passivation of industrial p-type Si PERC above 19%," Prog. Photovoltaics **20**, 269–273 (2012).

[14]S. Banerjee and M. K. Das, "A review of Al_2O_3 as surface passivation material with relevant process technologies on c-Si solar cell," Opt. Quantum Electron. **53**, 60 (2021).

[15]B. F. Bory, H. L. Gomes, R. A. J. Janssen, D. M. de Leeuw, and S. C. J. Meskers, "Electrical conduction of LiF interlayers in organic diodes," J. Appl. Phys. **117**, 155502 (2015).

[16]F.-C. Chiu, "A review on conduction mechanisms in dielectric films," Adv. Mater. Sci. Eng. **2014**, 578168.

[17]E. H. Nicollian and J. R. Brews, *MOS (Metal Oxide Semiconductor) Physics and Technology* (John Wiley and Sons, 1982).

[18]K. Piskorski and H. M. Przewlocki, "The methods to determine flat-band voltage VFB in semiconductor of a MOS structure," in *The 33rd International Convention MIPRO* (IEEE, 2010), pp. 37–42.

[19]G. Brammertz, T. Kohl, J. de Wild, D. G. Buldu, G. Birant, M. Meuris, J. Poortmans, and B. Vermang, "Bias-dependent admittance spectroscopy of thin-film solar cells: Experiment and simulation," IEEE J. Photovoltaics **10**, 1102–1111 (2020).

[20]J. Parion, R. Scaffidi, D. Flandre, G. Brammertz, and B. Vermang, "Low-temperature admittance spectroscopy for defect characterization in $Cu(In,Ga)(S,Se)_2$ thin-film solar cells," in *20th International Conference on Smart Technologies (IEEE EUROCON 2023)* (IEEE, 2023), pp. 99–104.

[21]J. Parion, "Opto-electrical characterization and modelling of defects in thin-film $Cu(In,Ga)Se_2$ solar cells," Master's thesis (University of Louvain, Belgium, 2022).

[22]R. Kotipalli, R. Delamare, O. Poncelet, X. Tang, L. A. Francis, and D. Flandre, "Passivation effects of atomic-layer-deposited aluminum oxide," EPJ Photovoltaics **4**, 45107 (2013).

[23]R. Scaffidi, D. G. Buldu, G. Brammertz, J. de Wild, T. Kohl, G. Birant, M. Meuris, J. Poortmans, D. Flandre, and B. Vermang, "Comparative study of Al_2O_3 and HfO_2 for surface passivation of $Cu(In,Ga)Se_2$ thin films: An innovative Al_2O_3/HfO_2 multistack design," Phys. Status Solidi A **218**, 2100073 (2021).

[24]S. M. Sze and K. K. Ng, *Physics of Semiconductor Devices*, 3rd ed. (Wiley-Interscience, Hoboken, NJ, 2007).

[25]L. Black, *New Perspectives on Surface Passivation: Understanding the Si-Al_2O_3 Interface*, Springer Theses (Springer, Germany, 2016).

[26]C. León, J. M. Martin, J. Santamaría, J. Skarp, G. González–Díaz, and F. Sánchez–Quesada, "Use of Kramers–Kronig transforms for the treatment of admittance spectroscopy data of p–n junctions containing traps," J. Appl. Phys. **79**(10), 7830–7836 (1996).

[27]W. Fahrner, T. Mueller, M. Scherff, D. Knoner, and H. Neitzert, "Interface states of heterojunction solar cells," in *IEEE 4th World Conference on Photovoltaic Energy Conference* (IEEE, 2006), pp. 1160–1163.

[28]J. M. V. Cunha, M. A. Barreiros, M. A. Curado, T. S. Lopes, K. Oliveira, A. J. N. Oliveira, J. R. S. Barbosa, A. Vilanova, M. J. Brites, J. Mascarenhas, D. Flandre, A. G. Silva, P. A. Fernandes, and P. M. P. Salomé, "Perovskite metal–oxide–semiconductor structures for interface characterization," Adv. Mater. Interfaces **8**, 2101004 (2021).

[29]J. de Wild, R. Scaffidi, G. Brammertz, G. Birant, and B. Vermang, "Dielectric front passivation for $Cu(In,Ga)Se_2$ solar cells: Status and prospect," Adv. Energy Sustainable Res. **4**, 2200132 (2023).